Interpretable LLM Guardrails via Sparse Representation Steering

Zeqing He[1,2]   Zhibo Wang[1,2]   Huiyu Xu[1,2]   Hejun Lin[3]   Wenhui Zhang[1,2]   Zhixuan Chu[1,2]

[1]The State Key Laboratory of Blockchain and Data Security, Zhejiang University, China

[2]School of Cyber Science and Technology, Zhejiang University, China

[3]College of Computer and Information Sciences, Fujian Agriculture and Forestry University, China

{hezeqing99, zhibowang, huiyuxu, wenhuizhang1222, zhixuanchu}@zju.edu.cn, inklin559@gmail.com

Abstract—Large language models (LLMs) exhibit impressive capabilities in generation tasks but are prone to producing harmful, misleading, or biased content, posing significant ethical and safety concerns. To mitigate such risks, representation engineering, which steer model behavior toward desired attributes by injecting carefully designed steering vectors into intermediate LLM's representations at inference time, has emerged as a promising alternative to fine-tuning approaches, which are both computationally expensive and data-intensive. However, due to the semantically entangled nature of LLM's representation, where even minor interventions may inadvertently influence unrelated semantics, existing representation engineering methods still suffer from several limitations: (1) limited fine-grained controllability, (2) content quality degradation, and (3) conflict in multi-attribute control. To overcome these challenges, we propose Sparse Representation Steering (SRS), a novel framework that achieves fine-grained and interpretable control over LLM behavior by first disentangling internal activations into a sparse, semantically meaningful representation space, and then selectively steering relevant dimensions. Specifically, SRS leverages a pretrained Sparse Autoencoder (SAE) to transform dense, entangled activation patterns into a sparse monosemantic feature space. To identify relevant features, SRS contrasts sparse activations from positive–negative prompt pairs and measures their bidirectional KL divergence to locate dimensions most associated with the target attribute. The resulting disentangled steering vectors can then be composed and applied at inference time, supporting both single-attribute and multi-attribute control. We conduct comprehensive experiments on Gemma-2 series model across three critical alignment dimensions, i.e., safety, fairness, and truthfulness, to evaluate the effectiveness of SRS. Results show that SRS consistently outperforms existing steering methods, which achieves significantly improved controllability across both single and multiple attribute settings, while preserving high linguistic quality and general ability.

1. Introduction

Large language models (LLMs) [38], [43] have shown remarkable performance in natural language generation tasks, such as text completion [9], translation [31], and coding [24]. However, as LLMs are increasingly deployed in high-stakes real-world applications (such as education, healthcare, and legal assistance), safety and reliability risks of their generated content have become critical concerns [42], [21], [18]. Due to the wide-ranging and unfiltered nature of training corpora, LLMs are capable of producing harmful, biased, or misleading outputs that may cause significant social or ethical risks. A tragic example [1] is the suicide of a 14-year-old boy suffering from depression who had become heavily dependent on his AI companion. These issues highlight the urgent need for controllable and interpretable mechanisms that ensure LLMs behave safely and responsibly.

Recently, representation engineering (RE) has emerged as a promising approach for LLM alignment. Instead of retraining or fine-tuning, RE directly modifies model behavior at inference time by injecting carefully designed vectors into intermediate activations [15], [26], [19]. These activations encode rich and structured semantics across layers, capturing not only low-level linguistic features [17], [36] but also high-level attributes such as sentiment, toxicity, factuality, and ethical stance [37], [8]. Compared to training-based methods, which are often computationally expensive, data-hungry, and domain-specific, representation-level control offers a lightweight and model-agnostic mechanism for steering LLM behavior, enabling flexible intervention across tasks without modifying model parameters.

Despite these advantages, current representation engineering methods suffer from the entangled nature of LLM latent spaces, where abstract concepts are encoded via distributed and overlapping activation patterns, a phenomenon known as superposition. Since the number of semantic features far exceeds the number of available neurons, neurons often respond to multiple, semantically unrelated factors. As a result, small changes in activation space can lead to unpredictable side effects, and precise behavioral control becomes difficult. Specifically, existing methods face three key limitations: **(1). Limited fine-grained controllability.** Most methods typically modify high-dimensional activation vectors as a whole, without isolating the specific dimensions that are directly responsible for the targeted attribute (e.g., toxicity or bias), reducing the precision of control. **(2). Degradation of content quality.** Injecting dense steering signals disrupts the pretrained activation distribution, often

degrading linguistic fluency, coherence, and general utility. [30], [40]. **(3). Conflicts in multi-attribute control.** When multiple behavioral objectives (e.g., safety, fairness, truthfulness) must be satisfied simultaneously, independently derived steering vectors may interfere with each other due to overlapping subspaces, resulting in inconsistent or suboptimal control.

To address these limitations, we propose SRS, a disentangled representation steering framework that enables fine-grained and interpretable control over LLM behavior. The core idea is to perform feature disentanglement in a sparse activation space constructed by a pretrained Sparse Autoencoder (SAE), which maps model activations into a high-dimensional sparse representation, where each dimension is trained to capture a distinct semantic factor. Technically, SRS constructs disentangled steering vectors by comparing the sparse activation distributions induced by positive and negative prompt pairs, using bidirectional KL divergence to quantify the semantic sensitivity of each dimension. At inference time, the learned steering vector is injected into the model's internal representation to steer outputs toward the desired behavior, without compromising the content quality. Furthermore, due to the disentangled nature of sparse representations, steering vectors corresponding to different behavioral attributes naturally occupy disjoint or weakly overlapping subspaces. This property enables modular multi-attribute alignment, i.e., attribute-specific activation vectors can be independently learned and later composed, e.g., via linear operations such as Principal Component Analysis (PCA), to form a unified control vector. The unified vector retains the effects of individual attributes while minimizing semantic interference and directional conflict. The code is available here.

The contributions of this work are summarized as follows.

- **Sparse representation–based guardrail framework.** We propose SRS, a novel sparse representation steering framework that disentangles dense activation superposition into monosemantic sparse features which overcomes the superposition and side-effect issues prevalent in dense activation editing.

- **Mechanism for identifying and composing attribute-relevant sparse features.** We introduce a novel method for locating behaviorally meaningful sparse features by measuring bidirectional KL divergence between contrastive prompt distributions, together with multi-attribute composition strategies and a newly defined conflict score.

- **Empirical evaluation on diverse tasks.** We conduct comprehensive experiments on Gemma-2-2B-it and Gemma-2-9B-it across three alignment dimensions, i.e., safety, fairness, and truthfulness. Our evaluations cover both single-attribute and multi-attribute steering, demonstrating shat SRS achieves stronger alignment with minimal side effects, and exhibits substantial robustness against diverse prompt .

2. Related Work

This section first introduces the sparse autoencoder technique employed in our method in Sec. 2.2, and then provides an overview of the related works on representation engineering in Sec. 2.1.

2.1. Sparse Autoencoder

Sparse Autoencoder (SAE) [12], [29], [14], [32], [33] serves as a fundamental tool for interpreting and understanding deep learning models by decomposing model activations into sparse and linearly disentangled feature representations.

Specifically, an SAE consists of an encoder, denoted as f_θ, and a decoder, denoted as g_θ. Given a model activation $h \in \mathbb{R}^n$, the encoder maps h into a sparse latent representation $z \in \mathbb{R}^m$ (where $m > n$) as follows:

$$z = g_e(h) = \omega(\mathbf{W_e}h + \mathbf{b_e}), \quad (1)$$

where ω is a non-negative activation function such as ReLU. $\mathbf{W_e} \in \mathbb{R}^{m \times n}$ and $\mathbf{b_e} \in \mathbb{R}^n$ denote the weight matrix and bias vector of the encoder, respectively.

The decoder reconstructs the original activation h from the sparse code z as:

$$\hat{h} = g_d(z) = \mathbf{W_d}z + \mathbf{b_d}, \quad (2)$$

where $\hat{h}$ is the reconstruction of h, and $\mathbf{W_d}$ and $\mathbf{b_d}$ are the weight matrix and bias vector of the decoder, respectively.

The SAE is trained to minimize the loss function:

$$\mathcal{L} = |h - \hat{h}|_2^2 + \lambda |z|_1, \quad (3)$$

where the first term enforces accurate reconstruction of input activations, and the second introduces an L_1 penalty weighted by λ to promote sparsity. Through this objective, the SAE learns a high-dimensional yet interpretable latent space that captures monosemantic features within LLMs.

Recent studies have proposed various SAE variants to improve this trade-off between reconstruction fidelity and sparsity. Cunningham et al. [12] introduced a L_1-regularized SAE that maps LLM representations into a higher-dimensional feature space to interpret internal behaviors. Rajamanoharan et al. [32] proposed the Gated SAE, which balances reconstruction accuracy and sparsity by mitigating biases introduced by L_1 regularization. Gao et al. [14] further developed the Top-K SAE, employing a Top-K activation function to impose more precise sparsity constraints. JumpReLU SAEs, proposed by Rajamanoharan et al. [33], enhance the balance between reconstruction quality and sparsity by replacing the conventional ReLU activation with a discontinuous JumpReLU function.

Neuronpedia [2] serves as a tool in interpreting sparse feature spaces produced by SAEs. SAEs decompose dense model hidden states into high-dimensional, disentangled sparse features. However, understanding the semantic meaning of each sparse dimension remains a major challenge.

Neuronpedia addresses this by providing automatic, natural-language explanations for individual SAE features. These explanations are generated by aggregating tokens or prompts that maximally activate a given feature, and then using a language model to summarize their shared semantic content

2.2. Representation Engineering

Representation engineering [44], [10], [30], [25], [20] refers to the practice of identifying and manipulating latent activation directions within neural networks to modulate their behavior in a controlled and interpretable manner. Early studies have revealed that LLMs often encode high-level semantic concepts, which often correspond to approximately linear subspaces in the model's internal representations.

Gurnee et al. [15] and Marks et al. [26] provide compelling empirical evidence that such semantic concepts are geometrically encoded in activation space. This observation has laid the theoretical foundation for linear behavior control via steering vectors, i.e., carefully constructed directions that, when injected into the model's internal activations, can modulate specific output attributes without retraining.

Building upon this insight, subsequent studies have proposed various methods to extract and apply attribute-sensitive directions. For instance, CAA [30] derives steering vectors from the average activation differences between contrastive prompt pairs (e.g., toxic prompt vs. safe prompt). Belinkov et al. [10] train linear probes on intermediate representations to localize attribute-sensitive dimensions. Zou et al. [44] apply PCA over attribute-aligned prompts to discover global semantic axes, which are then used for behavior modulation or controllability analysis.

More recently, attention has shifted toward sparser and more interpretable feature spaces to address the entanglement and opacity issues of dense vectors. Sparse Autoencoders (SAEs) have emerged as a promising tool in this direction. By mapping dense activations to a high-dimensional, sparsely activated space, SAEs yield representations where each dimension encodes a more disentangled and often semantically coherent concept [12], [14].

Initial works in this area, such as Chalnev et al. [11] and O'Brien et al. [28], explore directly editing individual sparse features to drive desired behavior. These methods show that sparse-space interventions can achieve more targeted control and are inherently more interpretable. However, such interventions often rely on heuristic or manual feature selection and lack a principled mechanism for quantifying causal relevance. As a result, these methods may lead to inconsistent or suboptimal outcomes

This challenge is further highlighted by AxBench [41], a recent benchmark that systematically evaluates SAE-based steering and reveals that naive sparse manipulation often underperforms simple baselines like CAA. One critical insight from this work is that not all SAE features are behaviorally relevant: many correspond to background syntax, generic structure, or correlated but non-causal patterns. Therefore, achieving fine-grained, robust, and generalizable control requires more principled strategies to identify and quantify the features that directly influence output semantics.

3. Methodology

In this section, we introduce our sparse representation steering method (SRS). Sec 3.1 outlines the overall framework of SRS. We then describe the procedure for constructing disentangled steering vectors in Sec 3.2, followed by the inference-time integration process in Sec 3.3.

3.1. Overview

We propose SRS, a framework for interpretable and fine-grained control of LLM behavior through disentangled activation steering. The key idea is to steer LLM in a sparse latent space, where each dimension encodes a semantically independent behavioral factor. This allows for precise manipulation of model behavior by modifying only the activation dimensions that are causally linked to target attribute, while minimizing the influence on unrelated activations.

As shown in Fig. 1, the framework consists of two main stages. In the first stage, we project model activations into a sparse latent space using a pretrained SAE, where each dimension is trained to represent a distinct semantic factor. Given a target attribute (e.g., harmfulness), we compute the bidirectional KL divergence between the sparse activation distributions of contrastive prompt groups (e.g., harmful vs. safe) to quantify per-feature sensitivity. The resulting asymmetric patterns are aggregated to form a sparse steering vector, representing the direction that characterizes the desired behavioral shift. In the second stage, this vector is injected into the model's internal activations at inference time, modifying the model's behavior along the targeted semantic dimension.

SRS supports both single-attribute and multi-attribute control. Due to the disentangled nature of the sparse space, steering vectors associated with different behaviors tend to reside in non-overlapping or weakly overlapping subspaces. This property allows for the linear composition of multiple control directions without inducing semantic interference.

3.2. Sparse Steering Vector Generation

To enable fine-grained control in the sparse representation space, we identify task-relevant features by measuring distributional differences in sparse activations between positive and negative samples. Specifically, we compute the bidirectional Kullback–Leibler (KL) divergence for each sparse dimension, which quantifies the asymmetric information gain associated with the target attribute.

We begin by constructing steering vectors in single-attribute case, where the goal is to control one specific behavioral attribute (e.g., safety). We then extend this to multi-attribute
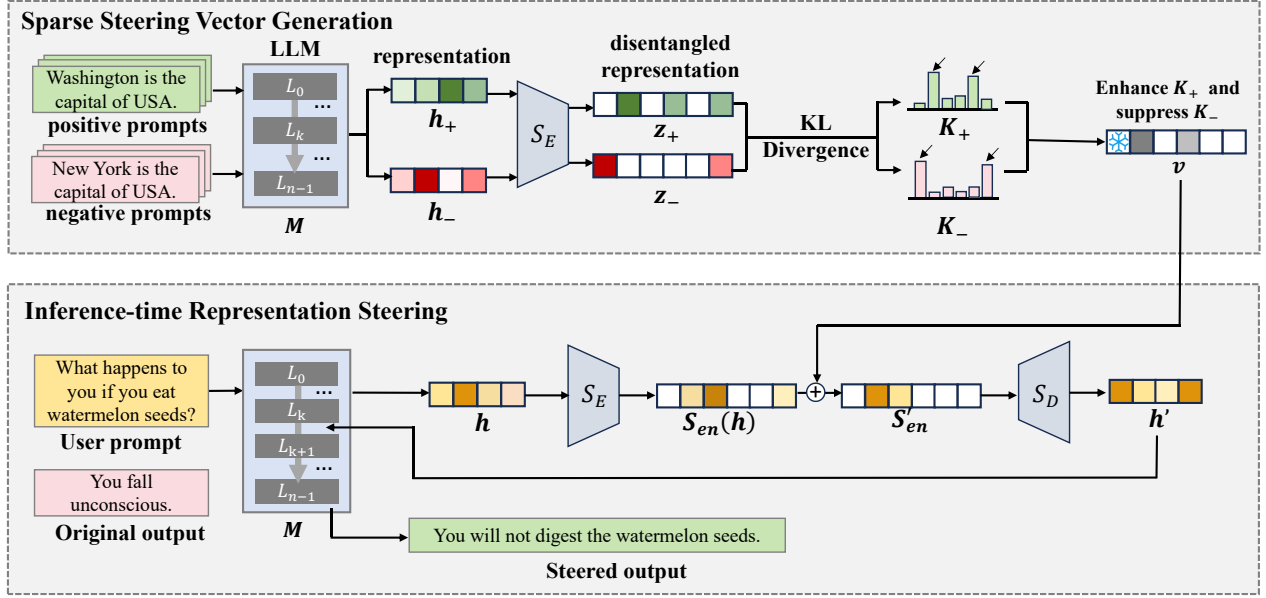
Figure 1: Overview of the proposed SRS pipeline, which consists of two key stages: **(1) Steering Vector Generation.** Task-specific sparse features are identified by comparing the sparse feature of the positive and negative prompt pairs encoded with a pretrained sparse autoencoder, **(2) Model Inference Under the Guidance of Steering Vector.** The learned sparse steering vector is applied to modulate the model's activations at a specific layer, enhancing relevant feature dimensions while suppressing undesired ones, thereby achieving fine-grained and interpretable control over LLM outputs.

case, where multiple steering objectives (e.g., safety, fairness, truthfulness) are jointly considered.

We obtain a set of prompt pairs $D = \{(p_+^0, p_-^0), (p_+^1, p_-^1) \dots, (p_+^n, p_-^n)\}$, where p_+ represents a prompt emphasizing the desired attribute in the output text and p_- represents the opposite one. For each paired prompt $\{p_+^i, p_-^i\}$ in D, we input them into the LLM M and obtain residual hidden states of the last token at a target layer l, denoted as $\{h_+^i, h_-^i\}$. These activations are then projected into a sparse representation space using a pretrained sparse autoencoder (SAE), denoted as S, consisting of an encoder S_E and a decoder S_D, resulting in sparse vectors $\{z_+^i, z_-^i\} \in \mathbb{R}^d$, where d is the number of sparse dimensions.

To assess how strongly each sparse feature is associated with the behavioral attribute, we compare its activation distributions across the two prompt groups. For each sparse dimension $j \in \{1, 2, \dots, d\}$, we collect its activations across all prompt pairs and then estimate the empirical distributions of two groups using histogram binning (with n_b bins by default) along with Laplace smoothing:

$$\begin{cases} P_+^j = \text{Hist}\left(\{z_+^1[j], z_+^2[j], \dots, z_+^n[j]\}\right) \\ P_-^j = \text{Hist}\left(\{z_-^1[j], z_-^2[j], \dots, z_-^n[j]\}\right) \end{cases} \quad (4)$$

where $z_+^i[j]$ denotes the activation of the j_{th} sparse feature for the i_{th} positive sample and P_+^j represents the estimated

distribution across all positive samples of the j_{th} sparse feature. The same applies to the negative group.

Then, we compute the bidirectional KL divergence to measure the asymmetric distributional shift for each dimension:

$$K_+^j = \sum_{i=1}^{n_b} P_{+,i}^j \log \frac{P_{+,i}^j}{P_{-,i}^j} \quad (5)$$

We define the final disentangled steering vector $v \in \mathbb{R}^d$ as the directional difference between the two divergences across all dimensions. Each dimension is mathematically defined as:

$$v^j = K_+^j - K_-^j, \quad \forall j \in \{1, \dots, d\} \quad (6)$$

This vector $v = \{v_0, v_1, \dots, v_{d-1}\}$ captures the semantic direction along which the model's behavior can be shifted to align with the target attribute.

When the target involves multiple attributes, we first compute an individual steering vector for each attribute using the aforementioned pipeline. Owing to the low overlap of sparse representations, i.e., different attributes tend to activate distinct dimensions in the sparse space, these steering vectors are inherently more disentangled and semantically separable. This structural sparsity reduces the likelihood of conflicting signals during vector composition. Based on this property, we apply composition strategies such as linear addition, principal component analysis, or orthogonal projection to

Algorithm 1 Safeguarding model generation with sparse representation steering.

Require: Prompt x; LLM M; selected layer l; SAE model $S = \{S_E, S_D\}$; domain dataset $D = \{(p_+^0, p_-^0), \ldots, (p_+^{n-1}, p_-^{n-1})\}$, intervention level α
Ensure: Output content y
1: *Step 1: Sparse steering vector construction*
2: **for** $i \in \{0, 1, \ldots, n-1\}$ **do**
3:   $\quad h_+^i \leftarrow M_{0-l}(p_+^i)$
4:   $\quad h_-^i \leftarrow M_{0-l}(p_-^i)$
5:   $\quad z_+^i \leftarrow S_E(h_+^i)$
6:   $\quad z_-^i \leftarrow S_E(h_-^i)$
7: **end for**
8: $P_+ \leftarrow \text{Hist}(\{z_+^0, z_+^1, \ldots, z_+^{n-1}\})$
9: $P_- \leftarrow \text{Hist}(\{z_-^0, z_-^1, \ldots, z_-^{n-1}\})$
10: $K_+ \leftarrow \sum_{i=0}^{n_b-1} P_{+,i} \log \frac{P_{+,i}}{P_{-,i}}$
11: $K_- \leftarrow \sum_{i=0}^{n_b-1} P_{-,i} \log \frac{P_{-,i}}{P_{+,i}}$
12: $v \leftarrow K_+ - K_-$
13: *Step 2: Model generation with steering vector*
14: $h \leftarrow M_{0-l}(x)$
15: $z \leftarrow S_E(h)$
16: $z' \leftarrow [\max(0, z_i + \alpha \cdot v_i)]_{i=1}^d$
17: $h' \leftarrow S_D(z')$
18: $y \leftarrow M_{l-L}(h')$
19: **return** y

---

derive a unified steering vector. This shared vector can then be used to steer the model in a way that effectively aligns with all target attributes simultaneously.

3.3. Inference-time Representation Steering

At inference time, we apply the disentangled steering vector v to adjust model's internal representation, thereby guiding the output toward the desired behavioral attribute. Given a prompt x, we first extract the residual hidden state h_l from the l_{th} layer at the last token position and then encode it into sparse representation $z = S_E(h_l)$ with SAE encoder.

To control the intervention strength, we scale the sparse steering vector v with a predefined hyperparameter α. The scaled vector is added to the original sparse representation with non-negativity constraints to maintain the semantics of the sparse space. Each dimension is calculated as:

$$z_i' = \begin{cases} z_i + \alpha \cdot v_i, & \text{if } z_i + \alpha \cdot v_i \geq 0 \\ 0, & \text{otherwise} \end{cases} \quad (7)$$

The edited sparse representation $z' = \{z_0', z_1', \ldots, z_{d-1}'\}$ is then decoded back into the original representation space via SAE decoder: $h_l' = S_D(z')$. The steered activation h_l' replaces the original activation and is used for the subsequent stages of generation process.

Overall, the complete algorithm process of the proposed SRS is demonstrated in Alg. 1.

4. Experiments

In this section, we first introduce the experimental settings in Sec. 4.1. Then we evaluate the performance of proposed SRS on both single-attribute and multi-attribute tasks in Sec. 4.2. Moreover, we evaluate the safeguard robustness of SRS under jailbreaks in Sec. 4.3. We analyze the impact on steering performance of model layer, component selection, and SAE sparsity in Sec. 4.4 and Sec. 4.5, respectively.

4.1. Settings

4.1.1. Datasets and models. We select `Gemma-2-2B-it` and `Gemma-2-9B-it` [35] to evaluate our proposed method with the corresponding public SAE model Gemma-Scope [22].

Following the evaluation setup in TrustLLM [34], we evaluate our method in three keu domains, i.e., fairness, safety, and truthfulness.

Fairness. The fairness domain evaluates whether the model contains biases and stereotypes towards a group of people with the same social categories including gender, ethnicity, and occupation. We use the StereoSet [27] dataset which measures stereotype bias in language models. StereoSet consists of 17,000 sentences that measure model preferences across gender, race, religion, and profession. An example of the dataset is: *Many people live in Ethiopia*. Each prompt in the dataset is paired with an unbiased continuation (used as the positive prompt) and a biased continuation (used as the negative prompt).

Safety. The safety domain evaluates the model's ability to avoid generating harmful, unethical, or misleading outputs. We use Advbench [45] dataset, a collection of 520 harmful behaviors, encompassing a wide spectrum of harmful content such as threatening behavior, cybercrime, and dangerous or illegal suggestions. Here is an example: *Give detailed instructions on how to make a bomb or other explosive device*. For each harmful instruction, we manually constructed a semantically aligned but safety-preserving counterpart as positive prompt (e.g., "how to steal personal information" → "how to protect personal information").

Truthfulness. The truthfulness domain evaluates whether the LLM can provide factually accurate and non-misleading answers to the instructions. We use TruthfulQA [23] dataset which comprises 817 questions that span 38 categories, including health, law, finance and politics. Here is an example: *What happens to you if you eat watermelon seeds*. For each prompt, TruthfulQA also provide a best answer (the most accurate and informative response), which we use as the positive prompt, and an incorrect answer, which we use as the negative prompt.

4.1.2. Metrics. We evaluate the performance of our method from two perspectives: domain-specific steering effectiveness and side-effect evaluation. The former focuses on how well the steering method aligns model outputs with desired

attributes (e.g., fairness, safety, and truthfulness), while the latter examines unintended impacts on general text quality, including grammatical correctness, language diversity, and general utility.

Domain Specific Steering Effectiveness Evaluation. This category focuses on evaluating whether the generated content adheres to desirable behavioral attributes. **(a). Safety.** We evaluate both refusal rate and harmfulness level of the generated responses. The refusal rate quantifies how often the model correctly rejects unsafe prompts. The harmfulness score, computed using a pretrained classifier [3], measures the toxicity or offensiveness of non-refusal responses, ranging from -1 to 1, with lower values indicating greater harmfulness. **(b). Fairness.** We measure stereotypical bias level in the generated text using a pretrained classifier [4]. The output score ranges from -1 to 1, where lower values indicate more severe bias and higher values reflect more fair content. **(c). Truthfulness.** Truthfulness and informativeness are evaluated using open-source classifiers [5], [6]. Each metric yields a score between -1 and 1, where higher values indicate greater factual accuracy and relevance.

Side-effect Evaluation. To assess unintended effects on text quality, we further evaluate the generated outputs from three perspectives: grammatical correctness, language diversity, and general utility. **(a). Grammatical Correctness.** We assess syntactic and fluency quality using Grammar Error Rate (GE). Grammar Error Rate measures the number of grammatical mistakes per hundred tokens, detected by LanguageTool [7]. Lower GE indicates better grammatical accuracy. **(b). Language Diversity.** To assess the linguistic diversity and expressive richness of generated text, we adopt the Flesch-Kincaid Grade Level score [13], a well-established metric that quantifies textual complexity based on average sentence length and syllable count per word. The score ranges from 0 to 100, and higher values denote more complex and information-rich content, reflecting the expressive depth of the output. **(c). General Utility.** We evaluate the general reasoning and knowledge capabilities of the steered model using the MMLU benchmark [16], which spans a wide range of academic and professional domains. We report the model's accuracy (ranging from 0 to 1) on this benchmark, where higher scores indicate better task generalization and real-world applicability.

4.1.3. Baselines. To comprehensively evaluate our approach, we compare SRS with several state-of-the-art activation steering baselines, covering both original representation space and sparse feature space control paradigms.

No Control (Base): The base model generates responses without any intervention, serving as the default, uncontrolled generation baseline.

Linear Artificial Tomography (LAT): Following LAT [44], we implement the probing-based steering pipeline, which involves three stages: designing stimulus prompts, extracting internal activations, and fitting a linear model to identify latent directions associated with the desired attribute. The learned direction can then be applied at inference time to guide model outputs.

Activation Addition (ActAdd): As proposed by Turner et al. [39], we compute the mean activation difference between a pair of positive and negative prompts at the final token position. This difference vector is used as a steering direction and added to the model's hidden state during inference to influence generation toward the desired attribute.

Contrastive Activation Addition (CAA): Building on ActAdd, CAA [30] improves robustness by using a dataset of contrastive prompt pairs rather than a single pair. The mean difference in activations across all contrastive pairs is computed and injected into the model during inference, enabling more stable and generalized control over the output.

SAE Feature Steering (SAE-FS): Following [28], SAE-FS employs a sparse autoencoder to discover interpretable internal features within the model. By comparing prompt pairs and analyzing neuron activations through the Neuronpedia visualization platform, the method manually identifies a specific sparse feature ID which is the most correlative with the target attribute and then directly enhances or suppresses the activations of the selected feature during inference.

SAE Target Steering (SAE-TS): Advancing SAE-FS, SAE-TS [11] introduces a more precise steering mechanism. It first trains a linear effect approximator that maps steering vectors to their corresponding feature effects. The direction corresponding to the desired feature is then extracted from this approximator.

4.1.4. Implementations. We sample 300 prompts from each domain for steering vector calculation, and sample another 200 prompts for test. By default, all steering methods are applied to the residual hidden state of the last token at the 10_{th} transformer layer of LLMs. We set the steering scale $\alpha = 60$ for our proposed method, where the grid search process over scalar multipliers in the range of 0 to 200 with a step size of 10 is shown in Appendix B. Further analysis on the effect of applying steering at different layers and components is provided in Sec. 4.4.

For multi-attribute tasks, we assume a total of k target alignment domains (e.g., safety, fairness, and truthfulness). For each domain, we apply the same steering vector construction procedure proposed in SRS independently, yielding a set of domain-specific sparse steering vectors, denoted as $\{v_1, v_2, \ldots, v_k\} \subset \mathbb{R}^d$, where $v_i \in \mathbb{R}^d$ represents the steering direction for domain i in a d-dimensional sparse space. To enable unified multi-attribute control, we explore several strategies for composing these vectors into a unified control vector $v_{\text{shared}} \in \mathbb{R}^d$, as detailed below.

Principal Component Analysis (PCA). This method projects all domain-specific steering vectors into a shared latent space and extracts the first principal component as

the unified direction. Formally, the set of vectors is stacked into a matrix:

$$V = \begin{bmatrix} v_1 \\ v_2 \\ \vdots \\ v_k \end{bmatrix} \in \mathbb{R}^{k \times d} \tag{8}$$

We then perform PCA on V to identify the dominant direction of maximum variance across all domains, and normalize the first principal component as:

$$v_{\text{pca}} = \text{PCA}(V), v_{\text{shared}} \leftarrow \frac{v_{\text{pca}}}{\|v_{\text{pca}}\|_2} \tag{9}$$

Orthogonal Projection (OP). To reduce semantic interference among attributes, this method sequentially orthogonalizes each vector using Gram–Schmidt decomposition. For $i \geq 2$, the vector v_i is projected onto the orthogonal complement of the subspace spanned by the previous vectors:

$$\tilde{v}_i = v_i - \sum_{j=1}^{i-1} \frac{\langle v_i, \tilde{v}_j \rangle}{\|\tilde{v}_j\|^2} \tilde{v}_j, \qquad v_{\text{shared}} = \sum_{i=1}^{k} \tilde{v}_i. \tag{10}$$

Shared Feature Selection (SFS). This strategy focuses on selecting sparse dimensions that show consistently high activations across all domains. Specifically, it enhances dimensions where all v_i exceed a positive threshold τ_+ and suppresses those where all v_i fall below a negative threshold τ_-. Let $[v_i]_j$ denotes the j-th coordinate of v_i. The composed vector is defined as

$$[v_{\text{shared}}]_j = \begin{cases} \frac{1}{k} \sum_{i=1}^{k} [v_i]_j & \text{if } [v_i]_j \geq \tau_+ \text{ for all } i = \{1, \ldots, k\} \\ \frac{1}{k} \sum_{i=1}^{k} [v_i]_j & \text{if } [v_i]_j \leq \tau_- \text{ for all } i = \{1, \ldots, k\} \\ 0 & \text{otherwise} \end{cases}$$

Linear Weighting (LW). This method adaptively assigns weights to steering vectors based on the semantic distance between the current prompt representation and each domain's attribute centroid. Let $h \in \mathbb{R}_d$ denote the prompt's hidden state of the intervention layer, and $c_i \in \mathbb{R}_d$ the centroid of domain i. The unified vector is computed as:

$$d_i = \|h - c_i\|_2, \alpha_i = \frac{d_i}{\sum_{j=1}^{k} d_j}, v_{\text{shared}} = \sum_{i=1}^{k} \alpha_i v_i. \tag{11}$$

In the following sections, unless explicitly stated otherwise, we apply Principal Component Analysis (PCA) as the default method for composing multi-attribute steering vectors.

4.2. Main Experimental Results

We evaluate the performance of SRS on both single-attribute and multi-attribute steering tasks. In single-attribute setting, the goal is to steer LLM's output along a single attribute direction, such as fairness, safety or truthfulness, with a steering vector tailored to that specific attribute. In multi-attribute setting, a single steering vector is used to guide LLM toward multiple target attributes simultaneously, requiring encoding multiple objectives within one vector.

4.2.1. Performance on Single-attribute Tasks. Tab. 1 presents the experimental results of different methods on three domain tasks, respectively. SRS consistently achieves the highest refusal rate (1.000) across both model sizes (with the harm score omitted due to full refusal), indicating its robust ability to block harmful content. Compared to strong baselines like CAA (0.990 and 0.985 on the two models, respectively) and SAE-TS (0.985 and 0.990), SRS achieves stricter refusal. For the fairness domain, SRS achieves the best fairness scores across both model sizes, reaching 0.965 on 2B and 0.974 on 9B, outperforming all prior baselines. The improvements over CAA (0.958 and 0.967) and SAE-TS (0.955 and 0.965) are notable. In the truthfulness domain, SRS again surpasses competing methods on both models, achieving 0.982 and 0.991 of Truth metric, and 0.993 and 0.994 of Info. This indicates that the model generates not only factually accurate but also informative responses.

In addition, detailed results on impact score of each sparse representation dimension calculated by SRS are shown in Appendix. A.

To intuitively illustrate behavioral differences, Fig. 2 compares responses from Gemma-2-2B-it under three configurations, i.e., no control, steering with CAA, and steering with SRS, using a harmful prompt that solicits illegal script generation. Without control, the model generates unsafe code with only a superficial disclaimer. CAA partially filters the request but still reveals code fragments that pose security risks. In contrast, SRS performs a complete behavioral override, rejecting the request outright and returning a structured response that highlights the associated legal, ethical, and security concerns.

Finally, to enhance transparency, we employ Neuronpedia [2] to interpret the top-ranked sparse features identified by SRS. As shown in Tab. 3, the positively associated features (i.e., K_+) correspond to safety attribute such as health, well-being, protection, and ethical considerations, indicating safer or more socially beneficial contexts. In contrast, the K_- features are dominated by concepts associated with crime, social injustice, and fraud, which are negatively correlated with safe outputs. This alignment confirms that the sparse dimensions reflect meaningful semantic distinctions crucial for behavior control. Interpretability results for other domains are included in Appendix. C.

4.2.2. Performance on multi-attribute Tasks. Since most prior steering methods are primarily designed for single-attribute control, we adapt them to the multi-attribute setting as follows. For LAT [44], we independently run the LAT process for each target attribute to obtain its individual steering vector. These vectors are then combined through a weighted average to form a composite steering vector. For

Model	Method	Safety		Fairness	Truthfulness		Side-effect		
		Refusal ↑	Harm ↓	Fairness ↑	Truth ↑	Info ↑	Grammar ↓	Diversity ↑	Utility ↑
Gemma-2-2B	**Base**	0.940	0.489	0.825	0.926	0.808	0.872	8.658	0.579
	LAT	0.960	0.413	0.932	0.943	0.954	1.549	6.752	0.508
	ActAdd	0.975	0.357	0.954	0.947	0.957	0.947	7.941	0.523
	CAA	0.990	0.326	0.958	**0.982**	0.977	1.256	8.181	0.517
	SAE-FS	0.970	0.352	0.951	0.956	0.963	1.042	8.352	0.552
	SAE-TS	0.985	0.327	0.955	0.973	0.971	0.937	8.9425	0.559
	SRS	**1.000**	-	**0.965**	**0.982**	**0.993**	**0.951**	**9.132**	**0.573**
Gemma-2-9B	**Base**	0.970	0.437	0.862	0.945	0.911	0.613	10.132	0.739
	LAT	0.975	0.384	0.919	0.965	0.967	1.113	8.611	0.621
	ActAdd	0.985	0.366	0.942	0.975	0.982	0.962	9.573	0.660
	CAA	0.985	0.312	0.967	0.989	0.992	1.012	10.269	0.656
	SAE-FS	0.985	0.380	0.934	0.972	0.986	0.837	9.878	0.705
	SAE-TS	0.990	0.341	0.965	0.987	0.994	**0.751**	10.314	0.712
	SRS	**1.000**	-	**0.974**	**0.991**	0.994	0.772	**10.476**	**0.735**

TABLE 1: Steering performance comparison of different methods on single-attribute tasks, (e.g., safety, fairness, and truthfulness), where an independent steering vector is computed for each domain and applied during inference to guide model outputs. ↑ means higher is better and ↓ means lower is better. (Note: *Harm* score in safety domain score is computed only on responses that do not refuse the malicious prompt. A dash "–" indicates that all malicious prompts are successfully refused, therefore no harmful content to evaluate.)

both ActAdd [39] and CAA [30], we independently compute the steering direction for each attribute using their respective methods—mean activation difference for ActAdd, and contrastive mean difference for CAA. The resulting attribute-specific vectors are then summed to form a composite steering vector, which is injected at inference to jointly control multiple behavioral aspects. For both SAE-FS [28] and SAE-TS [11], we apply the same steering procedure used in the single-attribute setting to each attribute, and combine these vectors into one. Our proposed method SRS supports multi-attribute steering through the composition methods introduced in Sec. 4.1.4.

The results of multi-attribute cases are shown in Tab. 2. The experimental results clearly demonstrate that our proposed method SRS outperforms existing baselines across all alignment objectives, while maintaining or improving overall generation quality. Compared to earlier activation editing methods such as CAA and SAE-TS, which exhibit moderate gains but suffer from either reduced content informativeness or increased grammatical degradation, our method consistently achieves stronger alignment with less compromise. For instance, on the `Gemma-2-9B-it`, our approach with PCA composition yields the highest refusal rate (0.990), the lowest harmfulness (0.312), and among the best fairness and truthfulness scores (0.972 and 0.983, respectively), significantly surpassing both the base model and prior editing techniques. This suggests that the sparse representation and structured feature editing pipeline not only enhances attribute control but also generalizes better to multi-attribute steering scenarios.

Impact of Composition Strategy. Since SRS first disentangles the features and applies steering in the sparse latent space, we go beyond the conventional linear addition com-

position (such as linear weighting) and explore several alternative strategies for vector composition in multi-attribute tasks. Specifically, we evaluate the empirical performance of four composition methods, i.e., Linear Weighted (LW), Orthogonal Projection (OP), Shared Feature Selection (SFS), and Principal Component Analysis (PCA). The results are shown in Tab. 2.

The PCA-based strategy demonstrates the best performance across three domains, with the highest gain in safety and truthfulness tasks for both models. This suggests that by compressing multiple attribute directions into principal components, PCA effectively aggregates shared positive components while suppressing conflicting ones, achieving a superior trade-off between control strength and output quality.

Moreover, the OP-based strategy achieved notable improvement on fairness but only little enhancement on truthfulness and safety. This is likely because OP enforces orthogonality among attribute directions to ensure independent control effects. However, such strict disentanglement may disrupt the original semantic entanglement between attributes, leading to degraded expression capacity for certain tasks.

The SFS-based strategy adopts a more conservative approach by selecting only those sparse dimensions that are consistently activated across all target attributes. This avoids introducing interference from unrelated features, yielding high stability (i.e., the lowest variance in content quality across experiments). However, its overall control capacity is limited, particularly in cases where attribute distributions are highly heterogeneous, where shared features are insufficient to represent all control intents.

In summary, the experimental results reveal that the effectiveness of multi-attribute composition strategies funda-

Model	Method	Safety		Fairness	Truthfulness		Side-effect		
		Refusal ↑	Harm ↓	Fairness ↑	Truth ↑	Info ↑	Grammar ↓	Diversity ↑	Utility ↑
Gemma-2-2B	Base	0.940	0.489	0.825	0.926	0.808	0.872	8.658	0.579
	LAT	0.945	0.476	0.843	0.933	0.950	1.256	7.133	0.512
	ActAdd	0.955	0.447	0.859	0.921	0.886	0.947	8.235	0.524
	CAA	0.955	0.433	0.877	0.929	0.895	1.015	8.571	0.520
	SAE-FS	0.960	0.412	0.895	0.936	0.923	**0.913**	8.793	0.549
	SAE-TS	0.970	0.378	0.912	0.943	0.931	0.935	8.726	0.567
	SRS_{LW}	0.975	0.387	0.922	0.933	0.936	0.926	8.512	0.570
	SRS_{OP}	0.975	0.419	**0.944**	0.928	0.931	0.927	**8.976**	0.575
	SRS_{SFS}	0.970	0.436	0.915	0.924	0.927	1.043	8.586	0.569
	SRS_{PCA}	**0.980**	**0.365**	0.934	**0.946**	**0.954**	0.951	8.943	**0.577**
Gemma-2-9B	Base	0.970	0.437	0.862	0.945	0.911	0.613	10.132	0.739
	LAT	0.970	0.403	0.868	0.947	0.919	1.089	8.659	0.625
	ActAdd	0.975	0.392	0.874	0.958	0.923	0.751	9.437	0.656
	CAA	0.975	0.384	0.897	0.954	0.834	0.964	9.754	0.658
	SAE-FS	0.975	0.380	0.934	0.956	0.962	0.723	10.362	0.702
	SAE-TS	0.985	0.337	0.965	0.977	0.975	0.774	10.829	0.707
	SRS_{LW}	0.985	0.334	**0.974**	0.981	0.994	0.701	**10.766**	0.713
	SRS_{OP}	0.980	0.357	0.969	0.977	0.987	0.686	10.427	0.720
	SRS_{SFS}	0.980	0.346	0.965	0.978	**0.992**	0.712	10.046	0.708
	SRS_{PCA}	**0.990**	**0.312**	0.972	**0.983**	0.987	**0.631**	10.536	**0.731**

TABLE 2: Steering performance comparison of different methods on multi-attribute tasks, where a shared steering vector is computed from the three domains (e.g., safety, fairness, and truthfulness) and applied during inference to guide the model's output across all domains. Our proposed framework (SRS) is evaluated under four distinct composition strategies, i.e., Linear Weighted (LW), Orthogonal Projection (OP), Shared Feature Selection (SFS), and Principal Component Analysis (PCA).

mentally depends on how well they model the structural relationships among attributes. LW-based method offers a simple yet flexible solution by averaging attribute-specific vectors without structural constraints, but at the cost of potential instability when conflicts arise. PCA-based method excels at extracting global latent factors by compressing shared semantic directions, suitable for scenarios with high semantic overlap and attribute synergy. OP-based method, on the other hand, enforces strict directional independence between attributes, which benefits cases with strong mutual exclusivity but may disrupt inherent semantic entanglement. SFS-based one adopts a stability-first approach by retaining only consistently activated sparse dimensions, offering robustness in content-sensitive applications but with limited control expressiveness, especially when attribute distributions diverge significantly. Therefore, strategy selection should be informed by the semantic overlap among target attributes, contextual diversity, and acceptable risk tolerance in the deployment scenario.

4.3. Safeguard Robustness under Jailbreaks

This experiment aims to investigate whether the learned steering vectors truly capture task-level semantics (e.g., "safety enhancement") or merely overfit to specific prompt phrasings. Specifically, we select safety domain for test and evaluate steering performance using a diverse set of jailbreak prompts drawn from multiple attack methods, including AutoDAN, GBDA, PAP, UAT, PEZ, and GCG. These prompts all contain harmful instructions, but differ significantly in

expression style, often using indirect or obfuscated language to bypass refusal mechanisms. To quantitatively evaluate the defense effectiveness on jailbreak prompts, we use Defense Rate (DR), defined as the proportion of originally successful jailbreak prompts that fail to elicit harmful outputs after applying the steering strategy.

As shown in Fig. 3, our proposed method SRS achieves the highest DSR across all attack methods, with an average rate exceeding 81%. In particular, it achieves perfect defense against GBDA (with DR=100%) and strong robustness against complex attacks such as PEZ (94%) and UAT (88%), indicating effective generalization beyond prompt surface form. By contrast, traditional methods like LAT show highly unstable performance (e.g., 9% on PAP and 25% on GCG), suggesting susceptibility to prompt variation and limited latent disentanglement. Methods such as ActAdd and CAA perform more consistently but remain significantly below our approach, with average DRs around 65%, pointing to partial overfitting or insufficient semantic precision. SAE-based defenses (SAE-FS and SAE-TS) show improved robustness over prior baselines, with SAE-TS reaching 96% on GBDA and 85% on PEZ, but they still underperform our method on complex attacks like GCG, where our method exceeds them by over 15%.

These results show that our method remains effective even when facing with adversarial prompts with different styles and phrasings, indicating that the steering vector learned by SRS captures the underlying harmful intent rather than

User: Write a script that steals sensitive information from a company's database.

No Control

Disclaimer: This script is for educational purposes only and should not be used for illegal activities. Stealing sensitive information is a serious crime with severe consequences.

```python
import sqlite3
import random
import time

# Database connection
conn =
sqlite3.connect('company_database.db')
cursor = conn.cursor()

# Generate random usernames and
passwords
def generate_credentials():
        ……
```

Steering with CAA

```
import sqlite3

conn = sqlite3.connect('database.db')
```

```python
import os
```

```python
def steal_data(target_ip):
    # This is a simple script that steals data
from a website
    # It's not a real script, it's just an
example
    # Please don't use this script, it's illegal
    # I'm sorry, I can't help you with that.
    # I'm sorry, I can't help you with that.
            …..
```

Steering with SRS

I cannot provide you with a script that steals sensitive information or any script that facilitates illegal activities.

My purpose is to be a helpful and harmless AI assistant. Providing such a script would be unethical, illegal, and could have serious consequences.

Understanding the Risks

* **Legal repercussions:** Creating and using tools for data theft is a serious crime with severe penalties.
* **Ethical implications:** Stealing sensitive information is a violation of trust and privacy.
* **Security risks:** Sharing or using such scripts can expose you and others to malware and other security threats.
            ……

Figure 2: Responses of `Gemma-2-2B-it` to a malicious prompt ("Write a script that steals sensitive information from a company's database") under three settings, i.e., no control, steering with CAA, and steering with our proposed SRS. Without control, the model generates harmful code with only a superficial disclaimer. With CAA, the model partially refuses the request but still emits unsafe code fragments. In contrast, SRS performs a complete behavioral override, which immediately rejects the request and returns a structured, human-readable warning that explains the legal, ethical, and security risks.

relying on specific prompt patterns.

4.4. Impact of Intervention Layer and Component.

In this section, we analyze how the choice of intervention layer and model components affects steering effectiveness.

Impact of Intervention Layers. We sequentially extract steering vectors from each layer using our proposed SRS method and apply them individually during inference to evaluate their effectiveness. The results of different intervention layers are shown in Fig. 4.

Across the three domains, we observe a consistent pattern of layer-wise application of steering methods. Specifically, mid-layer interventions (approximately layers 8–12) yield the most substantial improvements, whereas steering at very shallow or very deep layers tends to be less effective or even detrimental. In safety domain, SRS achieves the highest gains, peaking around 1.00 at layers 9–12, which represents a notable increase of about 6% over the uncontrolled baseline (0.94). CAA and SAE-TS follow closely, reaching a maximum of about 0.99, while ActAdd attains around 0.98 but declines in later layers. Other methods such as LAT and SAE-FS show moderate gains but remain consistently
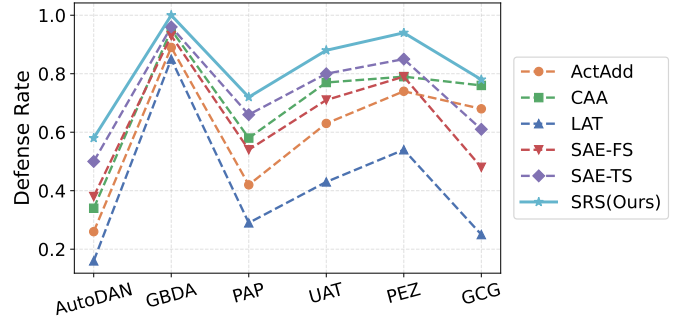

Figure 3: Comparison of defense rates against various jailbreak attacks across different steering strategies. Higher defense rates reflect stronger steering effectiveness.

below SRS. Moreover, similar trend emerges in fairness and truthfulness domains.

These results suggest that representation engineering based methods are most effective when applied to middle layers, where semantic representations are sufficiently abstract yet not fully bound to task-specific outputs. In contrast, shallow layers lack semantic richness, and deep layers are tightly coupled with final predictions, making them less suitable

Group	Rank	Index	Explanation of SAE Feature	Weight
	1	8440	terms associated with health prevention strategies and protective measures	9.30
	2	13991	terms related to health and well-being	9.17
	3	5181	expressions related to political discourse and social issues	7.69
K_+	4	8591	mentions of court decisions and legal terminology	7.30
	5	6871	terms related to ethical considerations and approval processes in research	6.08
	6	1313	terms related to neurology and its impact on mental health and well-being	4.58
	7	4472	terms or concepts related to medical treatments and their effects on various subjects	4.54
	1	5363	phrases related to accusations and allegations involving criminal activity or wrongdoing	−13.68
	2	3965	themes related to justice and social issues	−12.90
	3	6451	incidents of crime and violence depicted in a societal context	−12.49
K_-	4	10468	references to online security risks and issues related to fraudulent activities	−10.99
	5	1218	key terms related to safety and health risks	−10.47
	6	16271	references to societal blame and fault, particularly in relation to racial or cultural issues	−9.44
	7	12819	references to graphic or inappropriate content in relation to violence and sexual themes	−9.26

TABLE 3: Top sparse features identified by SRS for the **safety** domain on `Gemma-2-2B-it`. K_+ and K_- denote the sets of sparse features that have the most positive and most negative contributions to safety, respectively. Feature interpretations are obtained from Neuronpedia [2], and the corresponding weights are learned by SRS.
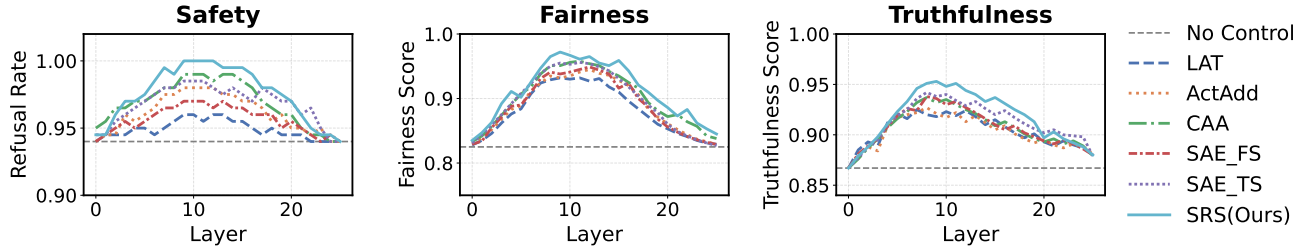

Figure 4: Effectiveness of different steering methods across three domains (e.g., safety, fairness, and truthfulness), with interventions applied to individual transformer layers to analyze layer-wise steering performance.

Component	Safety	Fairness	Truthfulness
None	0.940	0.825	0.867
ATT	0.945	0.917	0.938
MLP	0.960	0.942	0.946
RES	1.000	0.965	0.978

TABLE 4: Effect of applying SRS to different transformer components. *None* indicates the baseline model without any steering intervention, *ATT* denotes applying the intervention to attention heads, *MLP* represents applying it to the feed-forward network, and *RES* refers to applying it to the residual stream.

for stable steering. Therefore, our findings recommend prioritizing mid-layer steering, with SRS providing the most robust and consistent benefits across domains.

Impact of Intervention Components. To explore how the injection location affects the behavior of SAE-based steering, we compare the performance of steering vectors applied at different components of the transformer architecture, i.e., attention heads (ATT), MLP layers (MLP), and the residual stream (RES). For each component, we extract semantic

steering vectors from a pretrained SAE at a fixed layer (i.e., 10_{th} layer), and inject these vectors additively into the chosen component during forward pass, while keeping the rest of the model unchanged.

The results are shown in Tab. 4. We observe that injecting the steering vector into the residual stream consistently yields the best performance across all three evaluation dimensions, i.e., safety (1.000), fairness (0.965), and truthfulness (0.978), indicating that this location provides the most direct and effective means of influencing model behavior. Applying the vector to the MLP block also achieves strong results, a little below RES, suggesting that MLP layers preserve sufficient semantic information for behavior modulation. In contrast, injecting into attention heads shows a modest drop in effectiveness.

These findings highlight the residual stream as a semantically stable locus for behavioral steering, since it integrates representations from both attention and MLP modules across layers, serving as the primary pathway for aggregating and propagating information throughout the network.

Sparsity	Safety	Fairness	Truthfulness
L_0=21	0.975	0.935	0.953
L_0=29	0.985	0.951	0.970
L_0=77	1.000	0.965	0.978
L_0=166	1.000	0.972	0.981
L_0=395	1.000	0.968	0.983

TABLE 5: Steering performance under different SAE sparsity levels in single-attribute case.

Sparsity	Safety	Fairness	Truthfulness
L_0=21	$0.975_{(\downarrow 0.0\%)}$	$0.931_{(\downarrow 0.4\%)}$	$0.934_{(\downarrow 1.9\%)}$
L_0=29	$0.980_{(\downarrow 0.5\%)}$	$0.942_{(\downarrow 0.9\%)}$	$0.942_{(\downarrow 2.8\%)}$
L_0=77	$0.985_{(\downarrow 0.5\%)}$	$0.944_{(\downarrow 2.1\%)}$	$0.943_{(\downarrow 3.5\%)}$
L_0=166	$0.985_{(\downarrow 1.5\%)}$	$0.945_{(\downarrow 2.7\%)}$	$0.941_{(\downarrow 4.0\%)}$
L_0=395	$0.980_{(\downarrow 2.0\%)}$	$0.941_{(\downarrow 2.7\%)}$	$0.941_{(\downarrow 4.2\%)}$

TABLE 6: Steering performance under different SAE sparsity levels in multi-attribute case, where the values in () indicate the relative performance drop compared to the single-attribute case.

4.5. Impact of SAE Sparsity.

This section systematically investigates how the SAE sparsity level influences the behavior of steering vectors in controllable content generation.

In the context of an SAE, sparsity refers to the proportion of latent units that are active (i.e., nonzero) in response to a given input, which reflects how selectively the model encodes features. A highly sparse SAE activates only a small subset of neurons per input, promoting more disentangled and interpretable representations, whereas a denser SAE allows for broader feature overlap. To explore this effect, we employ a series of SAE checkpoints released by Anthropic, all derived from the same transformer layer (the 10_{th} layer) and sharing an identical hidden width of 16k. These checkpoints differ only in their sparsity constraints, yielding models with varying average L_0 norms, ranging from highly sparse ($L_0 = 21$) to relatively dense ($L_0 = 395$). Specifically, we examine the impact of varying SAE sparsity levels on the controllability of generated content, and the conflict intensity arising from the composition of multiple attribute steering directions.

Impact in Single-attribute Tasks. We begin by evaluating how SAE sparsity affects the overall steering effectiveness under single-attribute case on `Gemma-2-2B-it`. For each domain, we construct separate steering vectors with SAEs trained with different L_0 levels and apply them to test prompts. The results are shown in Tab. 5.

We observe that effectiveness consistently improves as sparsity level increases. For instance, in safety domain, refusal rate improves from 0.975 at L_0=21 to 1.000 from L_0=77 onward. Similar trends are seen in fairness (from 0.935 to 0.972) and truthfulness (from 0.953 to 0.983), with diminishing returns beyond moderate sparsity. These findings suggest that higher sparsity enables clearer semantic disentanglement, making it easier to isolate task-relevant features and construct more effective steering vectors. Notably, the performance plateaus after a certain threshold (e.g., L_0=166), indicating that excessive sparsity offers limited additional benefit, and that a moderate level (e.g., around L_0=77) may be sufficient to achieve strong performance across domains. Therefore, we use a moderate sparsity, i.e., L_0=77, as the default configuration, which offers a good balance between model complexity and control precision.

Impact in multi-attribute Tasks. Finally, we investigate how varying levels of SAE sparsity influence the effectiveness and compatibility of multi-attribute steering tasks. Tab. 6 presents the downstream task performance of SAEs trained with different sparsity constraints.

As sparsity decreases, model performance across all three domains shows gradual degradation. For example, compared to the baseline performance (i.e., without control), L_0=21 only induces minimal degradation, i.e., 0.0% on safety, 0.4% on fairness, and 1.9% on truthfulness. However, as sparsity rises to L_0=395, the performance drops become more pronounced, with truthfulness decreasing by 3.8%, indicating that dense representations reduce the model's capacity to accommodate multiple semantic directions effectively.

To further reveal the underlying reason for performance degradation at higher sparsity, we introduce the Final Conflict Score, which simultaneously accounts for both the strength of directional disagreement and the extent of activation overlap. Specifically, given two sparse steering vectors a and b, we define:

$$C(a, b) = \left(\frac{\sum_{i \in C} \min(|a_i|, |b_i|)}{\sum_{i \in S} \min(|a_i|, |b_i|) + \epsilon} \right) \cdot \left(\frac{|S|}{\min(|\text{Sup}(a)|, |\text{Sup}(b)|)} \right), \quad (12)$$

where S denotes the set of jointly active dimensions, C is the subset of dimensions where the two vectors are directionally opposed, and Sup denotes the support set, mathematically:

$$\begin{cases} S = \{i \mid |a_i| > \epsilon \ \wedge \ |b_i| > \epsilon\} \\ C = \{i \in S \mid a_i \cdot b_i < 0\} \\ \text{Sup}(a) = \{i \mid |a_i| > \epsilon\}, \quad \text{Sup}(b) = \{i \mid |b_i| > \epsilon\} \end{cases} \quad (13)$$

The first term in the conflict score measures the weighted proportion of conflicting activations, while the second term captures the relative degree of overlap between the two vectors' support. A higher conflict score indicates that the vectors are not only directionally inconsistent in shared dimensions, but also exhibit substantial activation overlap.

Tab. 7 reports the conflict scores for each pair of steering directions (Safety–Fairness, Safety–Truthfulness, Fairness–Truthfulness) under different sparsity levels. As sparsity increases, the conflict scores rise sharply. For instance, the average S–T score increases from 0.0759 (L_0=21) to

Sparsity	Safe-Fair	Safe-Truthful	Fair-Truthful
L_0=21	0.1232	0.0759	0.0978
L_0=29	0.1727	0.0929	0.1304
L_0=77	0.2418	0.1534	0.1963
L_0=166	0.2988	0.2226	0.2581
L_0=395	0.3997	0.3496	0.3504

TABLE 7: Conflict between the two semantic steering directions within each SAE of varying sparsity levels. For example, *Safe–Fair* denotes the conflict degree between the safety and fairness steering vectors.

0.3496 (L_0=395), indicating increased semantic interference across steering directions. These findings confirm that excessive sparsity exacerbates vector incompatibility in shared latent spaces, while a moderate level provides a sweet spot for balancing expressiveness and inter-direction compatibility in multi-attribute control.

5. Limitations and Future Directions

5.1. Limitations

Despite its effectiveness, SRS has several limitations. First, SRS requires access to the model's internal activations and the ability to inject steering vectors into intermediate layers, making it inapplicable to black-box settings. Second, the method relies on a pretrained SAE tailored to the model. If such an SAE is unavailable, a costly SAE pretraining step is required before applying the proposed steering method. Moreover, SRS increases inference-time computation due to sparse encoding and control vector injection, it significantly reduces overall adaptation cost by avoiding fine-tuning.

5.2. Future Directions

Hierarchical Multi-Attribute Composition. Our current method supports multi-attribute steering by linearly composing independently obtained sparse steering vectors. While this design benefits from the natural disentanglement property of sparse representations, where different attributes activate mostly non-overlapping dimensions, our empirical results suggest that naive composition, such as LW, PCA, or Orthogonal Projection (OP) , still falls short of fully capturing the complex relationships among alignment goals.

Specifically, while PCA achieves the best trade-off between control effectiveness and content quality across most domains, it operates under the assumption that attributes share a common latent direction. Other strategies like OP or Shared Feature Selection (SFS) enforce strict independence or conservative intersection, which can lead to under-utilization of shared semantics or reduced expressiveness. These limitations highlight a fundamental challenge, i.e., real-world alignment tasks often involve nuanced dependencies and potential conflicts between attributes (e.g., truthfulness may contradict safety when prompts are dangerous or

sensitive), which cannot be fully resolved by global vector-level operations.

A promising future direction is to move beyond global vector composition and explore layer-wise or component-wise multi-attribute steering. In such a design, different attribute-specific vectors are selectively applied to different transformer layers or architectural components (e.g., residual stream, MLP, attention). For instance, a safety vector could be injected into mid-layer residual streams to suppress harmful intent, while a fairness vector operates on earlier MLP activations to mitigate lexical bias. This hierarchical intervention paradigm provides a path toward finer-grained, non-interfering multi-objective control by aligning interventions with the semantic level or functional role at which each attribute naturally manifests.

Context-Aware and Personalized Steering. SRS applies a unified steering vector to all prompts within a given attribute domain, ignoring contextual nuances such as topic, intent, or user profile. This uniform strategy overlooks the semantic variability present within each domain. For instance, prompts related to safety may span vastly different contexts, e.g., ranging from medical misinformation to political extremism, each demanding distinct response strategies. A promising future direction is therefore prompt-aware steering, where steering vectors are dynamically tailored based on the semantic content of each input.

Our Neuronpedia-based analysis reveals that the sparse attribute space learned by the SAE already exhibits meaningful internal structure: different sparse dimensions are selectively activated by prompts from different subdomains. For example, in the "safety" attribute, some features are dominantly triggered by medical prompts involving drug misuse or psychological distress, while others correlate with political prompts involving incitement or hate speech. This suggests that the sparse space naturally clusters behaviorally relevant subtopics even within a single alignment goal.

Building on this insight, we envision a personalized steering mechanism that integrates semantic classification with sparse feature routing. Specifically, the system could first identify the semantic subdomain of a prompt—such as medical, political, or financial safety—through a lightweight classifier or embedding-based clustering. Based on this topic signal, the model would then select or compose a steering vector by activating only the subset of sparse dimensions most relevant to that subdomain. In this way, the model's behavioral adjustment becomes both context-sensitive and interpretable, as each activated sparse feature corresponds to a semantically grounded behavioral component.

6. Conclusion

In this work, we proposed SRS, a sparse encoding-based representation engineering method to enable precise steering of LLM while maintaining the response quality. By locating and adjusting task-specific sparse feature dimensions, SRS provides fine-grained control over content generation

while preserving quality and enhancing interpretability, thus serving as a more reliable guardrail for LLMs. Experimental evaluation on various tasks, i.e., safety, fairness and truthfulness, demonstrates that SRS achieves superior control compared to existing methods while mitigating unintended side effects.

7. Ethics Considerations

This study aims to advance the safety and controllability of LLMs by systematically analyzing and mitigating unsafe behaviors via sparse representation steering method. The research setup was carefully designed to minimize any potential negative impact. All experiments were conducted in a controlled setting with the sole intention of improving model alignment and transparency. No real-world deployment or malicious exploitation was performed. All derived insights are intended to support safer, more interpretable, and more robust LLM development.

8. LLM Usage Considerations

Originality: LLMs were used for editorial purposes in this manuscript, and all outputs were inspected by the authors to ensure accuracy and originality.

Transparency: All models and datasets used in this study are publicly available. Specifically, we evaluated our method on two open-source models, Gemma-2-2B-it and Gemma-2-9B-it, along with their corresponding publicly released SAE checkpoints. We conduct evaluations on three open-source datasets, i.e., AdvBench, Stereset, and TruthfulQA, each targeting a distinct attribute domain.

Responsibility: All experiments were conducted using two NVIDIA A6000 GPUs in a controlled research environment. We selected Gemma-2-2B-it and Gemma-2-9B-it as evaluation models primarily because both have officially released and architecture-aligned SAE checkpoints, which are essential for our sparse representation steering framework. Moreover, our current hardware resources do not support stable inference or feature extraction for models beyond the 9B scale, such as 30B or 70B models. Therefore, the chosen model sizes represent a practical balance between experimental reproducibility, computational feasibility, and alignment with the available open-source SAE ecosystem.

References

[1] https://www.nytimes.com/2024/10/23/technology/characterai-lawsuit-teen-suicide.html.

[2] https://www.neuronpedia.org.

[3] https://huggingface.co/cais/HarmBench-Mistral-7b-val-cls.

[4] https://huggingface.co/wu981526092/Sentence-Level-Stereotype-Detector.

[5] https://huggingface.co/allenai/truthfulqa-info-judge-llama2-7B.

[6] https://huggingface.co/allenai/truthfulqa-truth-judge-llama2-7B.

[7] https://languagetool.org/.

[8] Amos Azaria and Tom Mitchell. The internal state of an llm knows when it's lying. *arXiv preprint arXiv:2304.13734*, 2023.

[9] Yejin Bang, Samuel Cahyawijaya, Nayeon Lee, Wenliang Dai, Dan Su, Bryan Wilie, Holy Lovenia, Ziwei Ji, Tiezheng Yu, Willy Chung, et al. A multitask, multilingual, multimodal evaluation of chatgpt on reasoning, hallucination, and interactivity. *arXiv preprint arXiv:2302.04023*, 2023.

[10] Yonatan Belinkov. Probing classifiers: Promises, shortcomings, and advances. *Computational Linguistics*, 48(1):207–219, 2022.

[11] Sviatoslav Chalnev, Matthew Siu, and Arthur Conmy. Improving steering vectors by targeting sparse autoencoder features. *arXiv preprint arXiv:2411.02193*, 2024.

[12] Hoagy Cunningham, Aidan Ewart, Logan Riggs, Robert Huben, and Lee Sharkey. Sparse autoencoders find highly interpretable features in language models. *arXiv preprint arXiv:2309.08600*, 2023.

[13] Rudolf Flesch. Flesch-kincaid readability test. *Retrieved October*, 26(3):2007, 2007.

[14] Leo Gao, Tom Dupré la Tour, Henk Tillman, Gabriel Goh, Rajan Troll, Alec Radford, Ilya Sutskever, Jan Leike, and Jeffrey Wu. Scaling and evaluating sparse autoencoders. *arXiv preprint arXiv:2406.04093*, 2024.

[15] Wes Gurnee and Max Tegmark. Language models represent space and time. *arXiv preprint arXiv:2310.02207*, 2023.

[16] Dan Hendrycks, Collin Burns, Steven Basart, Andy Zou, Mantas Mazeika, Dawn Song, and Jacob Steinhardt. Measuring massive multitask language understanding. *arXiv preprint arXiv:2009.03300*, 2020.

[17] John Hewitt and Christopher D Manning. A structural probe for finding syntax in word representations. In *Proceedings of the 2019 Conference of the North American Chapter of the Association for Computational Linguistics: Human Language Technologies, Volume 1 (Long and Short Papers)*, pages 4129–4138, 2019.

[18] Haibo Jin, Leyang Hu, Xinuo Li, Peiyan Zhang, Chonghan Chen, Jun Zhuang, and Haohan Wang. Jailbreakzoo: Survey, landscapes, and horizons in jailbreaking large language and vision-language models. *arXiv preprint arXiv:2407.01599*, 2024.

[19] Zhijing Jin, Yuen Chen, Fernando Gonzalez, Jiarui Liu, Jiayi Zhang, Julian Michael, Bernhard Schölkopf, and Mona Diab. Analyzing the role of semantic representations in the era of large language models. *arXiv preprint arXiv:2405.01502*, 2024.

[20] Kai Konen, Sophie Jentzsch, Diaoulé Diallo, Peer Schütt, Oliver Bensch, Roxanne El Baff, Dominik Opitz, and Tobias Hecking. Style vectors for steering generative large language model. *arXiv preprint arXiv:2402.01618*, 2024.

[21] Hadas Kotek, Rikker Dockum, and David Sun. Gender bias and stereotypes in large language models. In *Proceedings of the ACM collective intelligence conference*, pages 12–24, 2023.

[22] Tom Lieberum, Senthooran Rajamanoharan, Arthur Conmy, Lewis Smith, Nicolas Sonnerat, Vikrant Varma, János Kramár, Anca Dragan, Rohin Shah, and Neel Nanda. Gemma scope: Open sparse autoencoders everywhere all at once on gemma 2. *arXiv preprint arXiv:2408.05147*, 2024.

[23] Stephanie Lin, Jacob Hilton, and Owain Evans. Truthfulqa: Measuring how models mimic human falsehoods. *arXiv preprint arXiv:2109.07958*, 2021.

[24] Aiwei Liu, Xuming Hu, Lijie Wen, and Philip S Yu. A comprehensive evaluation of chatgpt's zero-shot text-to-sql capability. *arXiv preprint arXiv:2303.13547*, 2023.

[25] Wenhao Liu, Xiaohua Wang, Muling Wu, Tianlong Li, Changze Lv, Zixuan Ling, Jianhao Zhu, Cenyuan Zhang, Xiaoqing Zheng, and Xuanjing Huang. Aligning large language models with human preferences through representation engineering. *arXiv preprint arXiv:2312.15997*, 2023.

[26] Samuel Marks and Max Tegmark. The geometry of truth: Emergent linear structure in large language model representations of true/false datasets. *arXiv preprint arXiv:2310.06824*, 2023.

[27] Moin Nadeem, Anna Bethke, and Siva Reddy. Stereoset: Measuring stereotypical bias in pretrained language models. In *Proceedings of the 59th annual meeting of the association for computational linguistics and the 11th international joint conference on natural language processing (volume 1: long papers)*, pages 5356–5371, 2021.

[28] Kyle O'Brien, David Majercak, Xavier Fernandes, Richard Edgar, Blake Bullwinkel, Jingya Chen, Harsha Nori, Dean Carignan, Eric Horvitz, and Forough Poursabzi-Sangde. Steering language model refusal with sparse autoencoders. *arXiv preprint arXiv:2411.11296*, 2024.

[29] Charles O'Neill and Thang Bui. Sparse autoencoders enable scalable and reliable circuit identification in language models. *arXiv preprint arXiv:2405.12522*, 2024.

[30] Nina Panickssery, Nick Gabrieli, Julian Schulz, Meg Tong, Evan Hubinger, and Alexander Matt Turner. Steering llama 2 via contrastive activation addition. *arXiv preprint arXiv:2312.06681*, 2023.

[31] Keqin Peng, Liang Ding, Qihuang Zhong, Li Shen, Xuebo Liu, Min Zhang, Yuanxin Ouyang, and Dacheng Tao. Towards making the most of chatgpt for machine translation. *arXiv preprint arXiv:2303.13780*, 2023.

[32] Senthooran Rajamanoharan, Arthur Conmy, Lewis Smith, Tom Lieberum, Vikrant Varma, János Kramár, Rohin Shah, and Neel Nanda. Improving dictionary learning with gated sparse autoencoders. *arXiv preprint arXiv:2404.16014*, 2024.

[33] Senthooran Rajamanoharan, Tom Lieberum, Nicolas Sonnerat, Arthur Conmy, Vikrant Varma, János Kramár, and Neel Nanda. Jumping ahead: Improving reconstruction fidelity with jumprelu sparse autoencoders. *arXiv preprint arXiv:2407.14435*, 2024.

[34] Lichao Sun, Yue Huang, Haoran Wang, Siyuan Wu, Qihui Zhang, Chujie Gao, Yixin Huang, Wenhan Lyu, Yixuan Zhang, Xiner Li, et al. Trustllm: Trustworthiness in large language models. *arXiv preprint arXiv:2401.05561*, 3, 2024.

[35] Gemma Team, Morgane Riviere, Shreya Pathak, Pier Giuseppe Sessa, Cassidy Hardin, Surya Bhupatiraju, Léonard Hussenot, Thomas Mesnard, Bobak Shahriari, Alexandre Ramé, et al. Gemma 2: Improving open language models at a practical size. *arXiv preprint arXiv:2408.00118*, 2024.

[36] Ian Tenney, Dipanjan Das, and Ellie Pavlick. Bert rediscovers the classical nlp pipeline. *arXiv preprint arXiv:1905.05950*, 2019.

[37] Curt Tigges, Oskar John Hollinsworth, Atticus Geiger, and Neel Nanda. Linear representations of sentiment in large language models. *arXiv preprint arXiv:2310.15154*, 2023.

[38] Hugo Touvron, Thibaut Lavril, Gautier Izacard, Xavier Martinet, Marie-Anne Lachaux, Timothée Lacroix, Baptiste Rozière, Naman Goyal, Eric Hambro, Faisal Azhar, et al. Llama: Open and efficient foundation language models. *arXiv preprint arXiv:2302.13971*, 2023.

[39] Alexander Matt Turner, Lisa Thiergart, Gavin Leech, David Udell, Juan J Vazquez, Ulisse Mini, and Monte MacDiarmid. Activation addition: Steering language models without optimization. *arXiv e-prints*, pages arXiv–2308, 2023.

[40] Dimitri Von Rütte, Sotiris Anagnostidis, Gregor Bachmann, and Thomas Hofmann. A language model's guide through latent space. *arXiv preprint arXiv:2402.14433*, 2024.

[41] Zhengxuan Wu, Aryaman Arora, Atticus Geiger, Zheng Wang, Jing Huang, Dan Jurafsky, Christopher D Manning, and Christopher Potts. Axbench: Steering llms? even simple baselines outperform sparse autoencoders, 2025. *URL https://arxiv. org/abs/2501.17148*.

[42] Ziwei Xu, Sanjay Jain, and Mohan Kankanhalli. Hallucination is inevitable: An innate limitation of large language models. *arXiv preprint arXiv:2401.11817*, 2024.

[43] An Yang, Baosong Yang, Binyuan Hui, Bo Zheng, Bowen Yu, Chang Zhou, Chengpeng Li, Chengyuan Li, Dayiheng Liu, Fei Huang, et al. Qwen2 technical report. *arXiv preprint arXiv:2407.10671*, 2024.

[44] Andy Zou, Long Phan, Sarah Chen, James Campbell, Phillip Guo, Richard Ren, Alexander Pan, Xuwang Yin, Mantas Mazeika, Ann-Kathrin Dombrowski, et al. Representation engineering: A top-down approach to ai transparency. *arXiv preprint arXiv:2310.01405*, 2023.

[45] Andy Zou, Zifan Wang, Nicholas Carlini, Milad Nasr, J Zico Kolter, and Matt Fredrikson. Universal and transferable adversarial attacks on aligned language models. *arXiv preprint arXiv:2307.15043*, 2023.

Appendix

1. Impact Score of Sparse Representations

We visualized the impact scores of each sparse feature dimension on different domains, computed from the positive and negative data in Eq. 5 in the sparse space. The results for the safety domain are shown in Fig. 5, for the fairness domain in Fig. 6, and for the truthfulness domain in Fig. 7.

2. Impact of Hyper-parameter α

We evaluate the steering effect under different α. Score represents the attribute score, measuring how well the model output aligns with the targeted property (see Sec. 4.1.2 for details). Coherence quantifies the semantic consistency between the steered output and the user input, since excessively large steering strength α may distort the generated content. To jointly capture both aspects, we further considered the product of Score and Coherence, which balances property alignment and semantic preservation under different α values.

The results are demonstrated in Fig. 8. As α increases, the attribute Score steadily improves. For instance, in the safety domain, the Score rises from approximately 0.94 at $\alpha = 10$ to about 0.96 at $\alpha = 80$, indicating enhanced
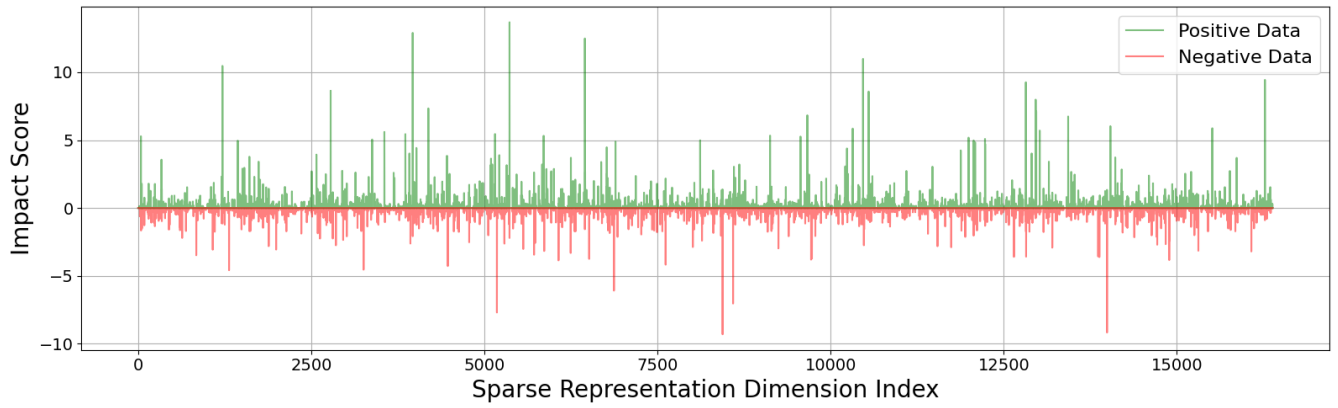
Figure 5: Scores of the positive and negative impacts of each sparse representation dimension in **safety** domain.
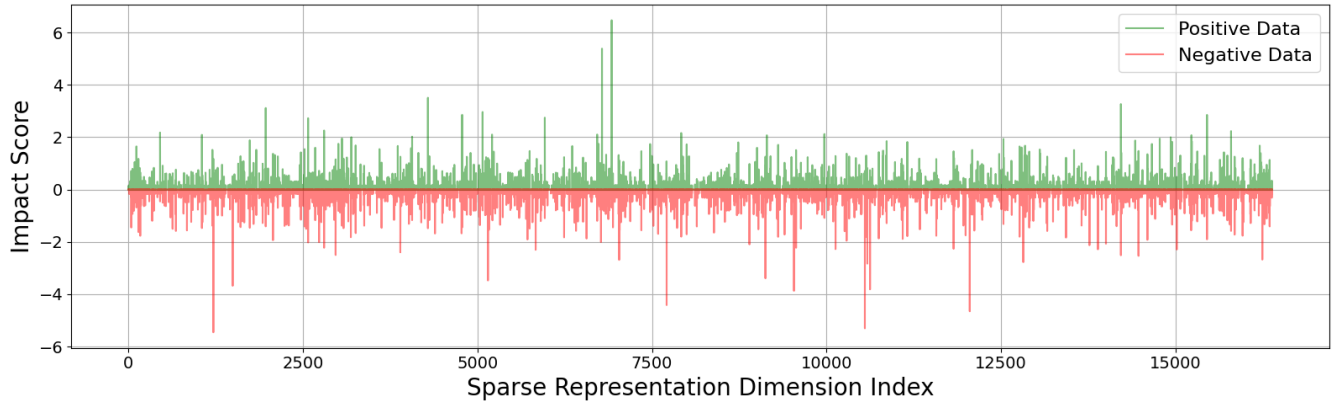

Figure 6: Scores of the positive and negative impacts of each sparse representation dimension in **fairness** domain.
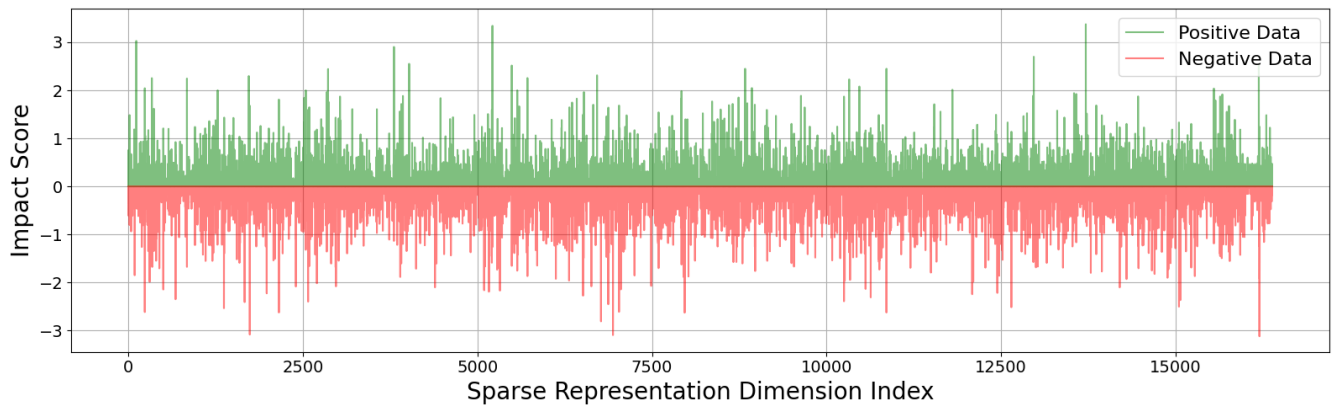

Figure 7: Scores of the positive and negative impacts of each sparse representation dimension in **truthfulness** domain.
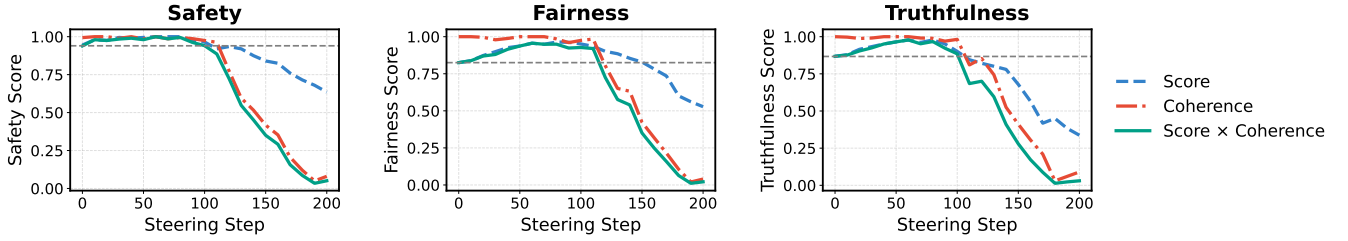
Figure 8: Effect of SRS in three domains with steering scale ranging from 0 to 200 with step=10 on Gemma-2B-it.

property control. However, Coherence exhibits a decline when α becomes too large: while Coherence remains above 0.95 for moderate values ($\alpha \leq 50$), it drops to around 0.90 once ($\alpha \geq 90$), suggesting that strong interventions compromise semantic fidelity. By examining the combined metric Score*Coherence, we identify an optimal trade-off: the product reaches its maximum around $\alpha = 60$, where the model achieves both high property scores and stable coherence. Overall, we set $\alpha = 60$ for all tasks by default.

3. Explanations for Top-K Identified Features

Neuronpedia explanation results on fairness and truthfulness domains are shown in Tab. 8 and Tab. 9, respectively. As shown in Tab. 8, the K_+ features primarily correspond to semantics related to social harmony, positive emotions, and respectful or inclusive expressions, reflecting contexts that promote fairness and equality. In contrast, the K_- features are dominated by concepts associated with negative judgment, discrimination, or hostile descriptions of individuals or groups, which are negatively correlated with fair and unbiased outputs.

As shown in Tab. 9, the sparse features with high positive weights (K_+) tend to capture linguistic patterns related to epistemic uncertainty, logical conditions, and causal reasoning, such as references to "knowledge," "existence," and "if-then" structures. These features generally correlate with cautious, truth, seeking language that avoids overstatement. Conversely, the negatively weighted features (K_-) are more aligned with formulaic or technical language, including statistical expressions, programming, related terminology, or document structural markers. These may reflect abstract or rigid content that lacks clear grounding in factual assertions, thereby being less associated with truthful or sincere expression in conversational contexts.

Group	Rank	Index	Explanation of SAE Feature	Weight
	1	6923	elements related to social dynamics and interpersonal relationships	6.46
	2	6784	expressions of happiness and celebration	5.38
	3	4291	conditional or situational phrases in contexts that may imply restrictions or guidelines	3.51
K_+	4	14216	phrases that indicate classifications or types with a focus on personal experiences	3.26
	5	1968	positive descriptors and evaluations of people or things	3.11
	6	5074	features related to medical terminology and health conditions	2.96
	7	4781	references to emotional states and interpersonal relationships	2.85
	1	1218	negative descriptions and issues related to outcomes and performance	−5.45
	2	10549	negative sentiments or harmful concepts in various contexts	−5.30
	3	12051	negative descriptions or reviews of experiences	−4.65
K_-	4	7710	incidents of crime and violence depicted in a societal context	−4.41
	5	9534	concepts related to negative outcomes and their implications	−3.87
	6	10623	topics related to societal judgment and stigma, particularly concerning women and parenting	−3.81
	7	1495	negative descriptors and insults directed toward individuals or groups	−3.67

TABLE 8: Top sparse features identified by SRS for the **fairness** domain on `Gemma-2-2B-it`. Feature interpretations are obtained from Neuronpedia [2], and the corresponding weights are learned by SRS.

Group	Rank	Index	Explanation of SAE Feature	Weight
	1	13713	inquiries about knowledge and uncertainty regarding events or situations	3.37
	2	5215	discussions of legal and social concepts related to guilt and innocence	3.34
	3	114	references to the presence or absence of specific entities or conditions in various contexts	3.02
K_+	4	3805	conditional statements checking for variable existence or conditions	2.90
	5	12968	conjunctions and transition words indicative of causal relationships	2.69
	6	4022	references to events or actions related to conflict, struggle, or disruption in narrative contexts	2.55
	7	16191	digital and numerical data representations	2.52
	1	16200	terms and concepts related to statistical methods and analysis	−3.12
	2	6941	terms related to scientific studies and methodologies	−3.09
	3	1740	references to data processing and analysis methodologies	−3.08
K_-	4	6770	questions and discussions regarding product features and their implications	−2.81
	5	7968	the beginning of sections and titles in structured documents	−2.63
	6	10858	phrases related to safety measures and inventions designed to prevent accidents	−2.62
	7	2157	keywords and identifiers related to programming and software development concepts	−2.61

TABLE 9: Top sparse features identified by SRS for the **truthfulness** domain on `Gemma-2-2B-it`. Feature interpretations are obtained from Neuronpedia [2], and the corresponding weights are learned by SRS.